Applied Thermal Engineering 71 (2014) 184–196

Contents lists available at ScienceDirect

Applied Thermal Engineering

journal homepage: www.elsevier.com/locate/apthermeng

Performance and environment as objectives in multi-criterion optimization of steam injected gas turbine cycles

Hasan Kayhan Kayadelen [a, b, *], Yasin Ust [a]

[a] Yildiz Technical University, Faculty of Naval Architecture and Maritime, Istanbul 34349, Turkey
[b] Princeton University, Department of Mechanical and Aerospace Engineering, Princeton, NJ 08544, USA

HIGHLIGHTS

- A thermodynamically precise performance estimation tool for GT cycles is presented.
- STIG application is provided to show its flexibility for any GT cycle and diluents.
- Constant TIT and net work output conditions have been compared and discussed.
- The model provides results to evaluate economic and environmental aspects together.
- It provides a precise estimation of adiabatic flame temerature and equilibrium species.

GRAPHICAL ABSTRACT

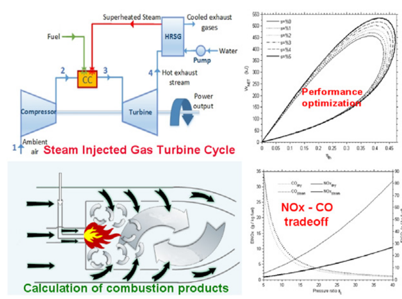

ARTICLE INFO

Article history:
Received 27 December 2013
Accepted 13 June 2014
Available online 3 July 2014

Keywords:
Gas turbines
Thermo optimization
Emissions
Engine simulation/modeling
Steam injection
Thermo-ecologic analysis

ABSTRACT

Rapidly growing demand for gas turbines promotes research on their performance improvement and reducing their exhaust pollutants. Even small increments in net power or thermal efficiency and small changes in pollutant emissions have become significant concerns for both new designs and cycle modifications. To fulfill these requirements an accurate performance evaluation method which enables to see the effects on the exhaust gas composition is an important necessity. To fill this gap, a thermo-ecologic performance evaluation approach for gas turbine cycles with chemical equilibrium approximation which enables performance and environmental aspects to be considered simultaneously, is presented in this work. Steam injection is an effective modification to boost power and limit NO_x emissions for gas turbine systems. Steam injection also increases thermal efficiency so less fuel is burnt to maintain the same power output. Because of its performance related and environmental advantages, presented approach is applied on the steam injected gas turbine cycle and a precise multi-criterion optimization is carried out for varying steam injection, as well as equivalence and pressure ratios. Irreversibilities and pressure losses are also considered. Effects of each parameter on the net work and thermal efficiency as well as non-equilibrium NO_x and CO emissions are demonstrated. Precision improvement of the presented thermo-ecological model is shown and two main concerns; constant turbine inlet condition for higher net work output and constant net work output condition for lower fuel consumption are compared.

* Corresponding author. Yildiz Technical University, Faculty of Naval Architecture and Maritime, Istanbul 34349, Turkey. Tel.: +90 212 383 29 42.
E-mail addresses: hasankayhankayadelen@hotmail.com, hkayhan@yildiz.edu.tr (H.K. Kayadelen).

http://dx.doi.org/10.1016/j.applthermaleng.2014.06.052
1359-4311/

1. Introduction

Gas turbine engines offer a wide range of power in relatively small sizes and are used in a variety of power generation purposes from utility power generation to transportation or military vehicles such as, airplanes, high-speed jets, helicopters, ships, tanks, locomotives and even in automobile and motorcycle turbochargers. As opposed to their competitor diesel engines, gas turbine engines can be operated on a wide range of fuels including natural gas which performs a cleaner combustion. The reason for this is that continuous-flow engines develop steady aerodynamics and flame kinetics which reduce the constraints placed on fuel properties for combustion such as limitations for RON (octane) number or cetane index. In addition, the fundamental characteristic of continuous combustion in a gas turbine engine is that the residence time at high flame temperatures (a key cause of NO_x formation) is capable of being controlled. A balance between smoke production and NO_x generation can also be easily secured [1–3]. According to some predictions gas turbines may furnish more than 80 percent of all new U.S. generation capacity in coming decades [4]. In addition to the advances in utility power generation, application of gas turbines in marine vessels have advanced significantly from only naval vessels in the 1970s to a broad range of commercial and new naval configurations [5]. Because gas turbines have wide operation flexibility and they meet an important portion of world's total energy demand their economic and ecological performance improvement have been significant concerns for the governments.

Although it is has long been realized that performance and emissions from gas turbines should be evaluated simultaneously, there are not more than a couple of analytical studies which investigate the performance of gas turbines together with their pollutant emissions. Some of them are given in Refs. [6–8]. Additionally, existing gas turbine models in the available literature treat the exhaust stream as air [9] or more precisely as a mixture of complete combustion products comprising of CO_2, H_2O, O_2 and N_2 only [8,10–18]. This simplifications will lack in precision although there is sufficient oxygen which can completely oxidize all the fuel because of the dissociations of combustion products at high temperatures. Some studies [19–24] use crude curve-fit equations or tables neglecting the type of fuel, equivalence ratio or effect of system pressure to calculate the properties of exhaust gas mixture. In some other studies exhaust gas properties are assumed to be constant regardless of changing temperatures and pressures [25–28]. Many studies also neglect the effect of pressure losses in gas turbine performance analysis [9,18,22,29]. Additionally, existing semi-analytical correlations [30–33] which are used by previous authors [8,23,28,34] to determine the levels of NO_x, CO and UHC need a very precise adiabatic flame temperature because all these pollutants are strongly dependent on adiabatic flame temperature especially NO_x. In these studies adiabatic flame temperature is calculated with the formula of Gülder [35] which is derived from curvefit data obtained from a chemical equilibrium code and which gives only approximate results in the case when steam is not present in the combustion chamber. This formula is not suitable for the case when steam is present in the combustion chamber i.e. to analyze steam injected gas turbines.

Heywood [36], Rashidi [37], Vissler and Kluiters [7] and Rakopoulos et al. [38], state that it is a good approximation for performance estimates in engines to regard the burned gases produced by the combustion of fuel and air as in chemical equilibrium and therefore knowledge of the exact gas composition inside the combustion chamber is critical for the accurate calculation of the thermodynamic cycle models of internal combustion engines. For this purpose a chemical equilibrium scheme is needed considering a certain number of species present inside the combustion chamber.

In this paper a more precise modeling approach is proposed which is based on calculating equilibrium exhaust species taking dissociations with temperature into account for estimation of thermodynamic properties of the working fluid and adiabatic flame temperature. In this paper adiabatic flame temperature is calculated using the exact equilibrium composition considering the effects of steam during combustion, so adiabatic flame temperature, accordingly the turbine inlet temperature and amounts of pollutants which strongly depend on adiabatic flame temperature are more precise than the previous works. Effect of this improvement to the adiabatic flame temperature and associated pollutant emissions can be seen in Table 2.

To obtain the equilibrium composition in steam injection case, the chemical equilibrium routines of Olikara and Borman [39] presented by Ferguson [40] were modified for H_2O injection and the equilibrium results obtained were compared with the results of computer programs GASEQ [41] and CHEMKIN [42]. The comparisons were quite satisfactory and presented at [43].

Proposed gas turbine model also takes pressure losses into account for better precision.

Many authors have investigated gas turbines and gas turbine cycles and have been working on their optimal emissions and performance [22–32]. Because steam injection makes considerable changes both on performance and NO_x emissions, steam/water injected internal combustion engines are of major concern for more than 30 years and scientist are still working on possible improvements of this well established development [8,11,18,44–51]. In steam injected gas turbines, maintaining a constant turbine inlet temperature increases the power output and thermal efficiency but increases the fuel consumption or the owner can elect to reduce fuel consumption and maintain the same nominal power output [4].

With the established model, thermodynamic properties of working fluid are calculated at all stations of a steam injected gas turbine cycle numbered in Fig. 1. Performance of the steam injected cycle is evaluated taking irreversibilities and pressure loses into account for varying steam injection, as well as equivalence and pressure ratios. Model results are compared with previous gas turbine models and improvements of the results are shown in Table 2. Effects of each parameter on the net work and thermal efficiency as well as non-equilibrium NO_x and CO emissions of the steam injected cycle are demonstrated. Two cases for steam injected gas turbines; constant turbine inlet temperature and constant net work output conditions which are preferred for increasing the net work output and lowering the fuel consumption respectively are examined and compared.

2. Modeling and simulation

A STIG cycle is depicted with its critical stations and dedicated station numbers in Fig. 1 and presented approach is used for the

Table 1
Gas turbine characteristic values for the simulation.

T_{amb} (°C)	15	η_{pump}	0.70
T_{fuel} (°C)	15	ΔP_{steam} (kPa)	405.3
T_{steam} (°C)	300	P_{in} (kPa)	101.325
TIT (°C)	1300	P_{exh} (kPa)	101.325
η_{cis}	0.87	P_{drop} (%)	0.04
η_{tis}	0.89	t_{res} (s)	0.002
η_{cc}	0.99	ϕ_{pri}	1.02

Table 2
Precision improvement of the presented approach.

Case nr.	0	1	2	3	1 + 2	2 + 3	1 + 2 + 3
Assumptions →	Proposed model	Four combustion products	Injected steam as ideal gas	No pressure loss	Four combustion products + steam as ideal gas	Injected steam as ideal gas + no pressure loss	Four combustion products + steam as ideal gas + no pressure loss
W_{NET}	522.22	532.86	522.44	530.27	532.61	530.157	529.68
η_{th}	0.4445	0.4542	0.4515	0.4603	0.4555	0.4610	0.4624
ϕ	0.3984	0.3976	0.3973	0.3907	0.3964	0.3902	0.3884
T_u	758.54	758.58	761.2	759.04	761.3	761.7	761.8
T_{ad}	2452.9	2511.9	2454.5	2453.2	2514.0	2454.4	2514.5
T_4	808.90	802.51	808.9	801.89	802.51	803.06	802.51
$EINO_x$	6.793	12.244	6.887	6.750	12.460	6.8344	12.395
EICO	4.931	4.197	4.922	Not applicable	4.187	Not applicable	Not applicable

thermo-ecologic performance analysis of the STIG cycle which is shortly described below:

In process 1–2, the compressor ingests the ambient air and pressurizes it to an elevated pressure depending on the engine design. Typically 50% or more of the work extracted by the turbine is used to drive the compressor as they are working dependently on the same shaft and the remainder is the useful work output. Compression is accompanied by an increase in air temperature. The hot compressed air then proceeds into the combustion chamber in process 2–3 where fuel is mixed with air and steam and then ignited, resulting in a continuous combustion process maintaining a further temperature rise.

Neglecting the small pressure losses, it is a constant-pressure process, since the chamber is open to flow, upstream and downstream. High quality steam, raised in a heat recovery steam generator (HRSG) is injected into the combustion chamber during the combustion process. The injected steam also increases the cycle efficiency with the increased mass flow rate through the turbine section of the gas turbine without any change in the compressor work. Furthermore, the specific heat of superheated steam is almost double that of air and the enthalpy of steam is higher than that of air at a certain temperature. This provides a significant augmentation in the net cycle work. The heated, pressurized and moisturized steady-flow gases at the turbine inlet temperature (TIT = T_3) then gives up its energy, expanding through the turbine in process 3–4. In simple open gas turbine cycles there is a path from 4 back to 1, a constant pressure cooling process which is done continuously by the atmosphere is done by the HRSG here.

The required pressure for the injected steam produced by HRSG which is assumed to be 4 bars above the combustion chamber pressure [52] is supplied by a pump which pressurizes water at ambient temperature. Calculations indicate that there is more than enough waste heat in the exhaust to produce this steam from the gas turbine hot exhaust gases [52]. As an example, Saravanamuttoo et al. states that a 40 MW aero-derivative gas turbine may only use about 25% of the steam produced in the HRSG to limit NO_x [53]. Poullikkas states that typically, gas turbines are designed to allow up to 5% of the compressor airflow for steam injection to the combustion chamber and compressor discharge [54]. This present work assumes that HRSG can produce up to 5% diluent by mass of the air supplied for the combustion m_{a1}.

For the analytical model used in the simulation, the following assumptions have been made:

– All gases except injected steam are ideal gases and their enthalpies and specific heats only change with temperature.
– The fuel selected for the particular analysis is pure methane (CH_4) and the combustion is adiabatic.
– The air supplied for the combustion is completely dry without any moisture and contains only 0.21 mol of O_2 and 0.79 mol of N_2.
– For the unburned air–fuel–steam mixture, the temperature of the reactant air is equal to the compressor outlet temperature and fuel temperature is assumed to be equal to the ambient temperature.
– The combustion is assumed to take place at stationary state and the combustion chamber is assumed to be a well stirred reactor (WSR) and primary zone residence time is assumed to be 0.002 s [28,55].

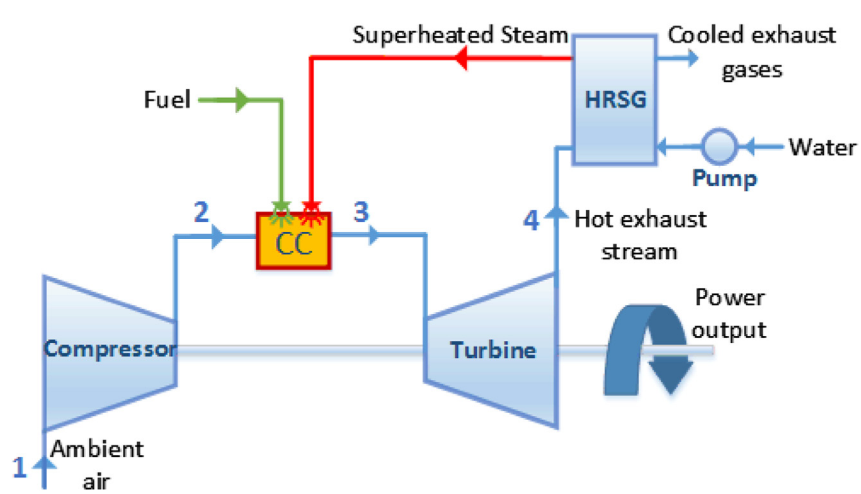

Fig. 1. Steam injected gas turbine cycle.

– Since only a small amount of diluent by volume is injected, the pressure [56] and concentrations of the reactants in the combustion chamber are assumed to remain unchanged.

Characteristic values for the gas turbine simulation are given in Table 1.

2.1. Compression analysis

Ambient temperature and pressure T_1 and P_1 are selected as 15 °C and 1.01325 bar which are the standard conditions used by the gas turbine industry established by ISO [57].

In order to determine the temperature of air at the compressor exit, the relative pressure of air at temperature T_1 is needed which can be taken from the isentropic properties of air tables [58–60] or directly calculated from the following equation:

$$Pr(T) = \exp\left[\frac{\bar{s}^o(T)}{\bar{R}_u}\right] \tag{1}$$

where $\bar{s}^o(T)$ is the molar absolute standard state of entropy of air at temperature T and $\bar{R}_u$ is the molar universal gas constant defined as follows:

$$\bar{R}_u = R_u M \tag{2}$$

Here, R_u denotes the universal gas constant equal to 8.31434 kJ/kmol K and M denotes the molecular weight of the gas or the gas mixture. Using Pr_1 and the compressor pressure ratio π_c, which is equal to P_2/P_1, $Pr_{2,is}$ is calculated as below:

$$Pr_{2,is} = Pr_1 \pi_c \tag{3}$$

The temperature of air after the ideal isentropic compression T_{2s} can now be obtained from the same tables finding the corresponding temperature for Pr_{2s} by means of linear interpolation or solving Eq. (1) for T. Using $T_{2,is}$, the actual compressor exit temperature T_2 can be calculated using the compressor isentropic efficiency $\eta_{c,is}$ as below:

$$T_2 = T_1 + \frac{T_{2,is} - T_1}{\eta_{c,is}} \tag{4}$$

The enthalpy of compressor inlet air h_1 and the enthalpy of compressor exit air for their corresponding temperatures are obtained by using curvefit coefficients $(a_1 \ldots a_n)$ for thermodynamic properties of (C–H–O–N) systems [61] for mole fractions of 0.21 O_2 and 0.79 N_2 so that h_1 and h_2 will be on the same reference with the combustion enthalpy h_3 which is going to be obtained from the combustion model.

For the performance estimation compressor and pump work should be calculated. The specific compressor work is obtained from the following relation:

$$w_C = h_2 - h_1 \tag{5}$$

and the pump work is calculated as below:

$$w_p = h_{pump_{out}} - h_{pump_{in}} = v_{sat}(P_{out} - P_{in})/\eta_{pump} \tag{6}$$

2.2. Combustion analysis

In steam injected gas turbines the control unit fixes the TIT to a constant predetermined value and consequently more fuel is injected into the combustion chamber with increasing steam injection ratios. Here a slightly moderate temperature, 1300 °C, is selected for the simulation and performance analysis which is held constant at different pressure ratios. Accordingly, fuel/air ratio decreases for increasing pressure ratios. Combined pressure loss in the combustion chamber due to friction, turbulence and temperature rise including the pressure loss in turbine is taken into account which is assumed to be 4% total.

Considering that for $\varphi < 3$ and there are 10 constituents, the high temperature combustion model with the reactant H_2O added is established by taking the equilibrium constants into account and the equilibrium products of combustion are calculated as a function of temperature and equivalence ratio as suggested by Ferguson [40]. The chemical equation for the combustion model is given below:

$$\begin{aligned}\varepsilon\phi C_\alpha H_\beta O_\gamma N_\delta + (0.21O_2 + 0.79N_2) + xH_2O \rightarrow v_1CO_2 + v_2H_2O \\ + v_3N_2 + v_4O_2 + v_5CO + v_6H_2 + v_7H + v_8O + v_9OH + v_{10}NO\end{aligned} \tag{7}$$

where ν_1 to ν_{10} represents the number of moles for each species, α, β, γ, δ are the numbers of carbon, hydrogen, oxygen and nitrogen atoms present in the fuel. ϕ is the overall equivalence ratio, ε is the molar air–fuel ratio obtained from the stoichiometric combustion of the fuel and x is the molar injection ratio of H_2O which are calculated as below:

$$\phi = \frac{FA}{FA_s} \tag{8}$$

$$\varepsilon = \frac{0.21}{\alpha + \frac{\beta}{4} - \frac{\gamma}{2}} \tag{9}$$

$$x = \frac{MW_{air}}{MW_{H_2O}} s \tag{10}$$

where s is the steam injection ratio which stands for m_s/m_a, which is an important parameter for introducing the performance of the steam/water injected cycle.

To solve for υ_i, 10 unknown mole numbers and obtaining the mole fractions y_i, the equilibrium method of Ferguson [40] is adapted for H_2O injection. In order to solve for the mole fractions of products of Eq. (7) and (11) equations are needed which 6 of them can be provided by the criteria of equilibrium among the products. There are four more equations which come from the combustion model atom balancing and one from definition of mole fraction $\sum y_i = 1$. Using both Gauss–Seidel and Newton–Raphson methods together would combine the speed of the first and the reliability of the latter is an efficient way which converge faster to an accurate solution of the equation set [62]. The reliability of this method has been proved comparing the solutions with the results of computer programs GASEQ [41] and CHEMKIN [42]. The details of this work are presented by authors at [43].

Molar specific heat, enthalpy and entropy values of each species can be obtained from following expressions by using curvefit coefficients $(a_1 \ldots a_n)$ for thermodynamic properties of (C–H–O–N) systems [61]:

$$\frac{\bar{h}_i^o}{R_u T} = a_{1,i} + \frac{a_{2,i}}{2}T + \frac{a_{3,i}}{3}T^2 + \frac{a_{4,i}}{4}T^3 + \frac{a_{5,i}}{5}T^4 + \frac{a_{6,i}}{T} \tag{11}$$

$$\frac{\bar{c}_{p,i}}{R_u} = a_{1,i} + a_{2,i}T + a_{3,i}T^2 + a_{4,i}T^3 + a_{5,i}T^4 \tag{12}$$

$$\frac{\bar{s}_i^0}{R_u} = a_{1,i} In\, T + a_{2,i}T + \frac{a_{3,i}}{2}T^2 + \frac{a_{4,i}}{3}T^3 + \frac{a_{5,i}}{4}T^4 + a_{7,i} \tag{13}$$

At constant pressure, enthalpy of the mixture change due to the dissociations as the mole fractions of the mixture change with temperature. This will change the ultimate specific heat of the gas mixture defined as follows:

$$h = \sum_{i=1}^{10} y_i \bar{h}_i^o \quad [\mathrm{kJ/kmol}]. \tag{14}$$

$$h = \frac{1}{M}\sum_{i=1}^{10} y_i \bar{h}_i^o \quad [\mathrm{kJ/kg}]. \tag{15}$$

$$\left(\frac{\partial h}{\partial T}\right)_P = c_{p_g} = \sum_{i=1}^{10} \frac{y_i}{M}\frac{\partial \bar{h}_i^o}{\partial T} + \frac{\bar{h}_i^o}{M}\frac{\partial y_i}{\partial T} - \frac{y_i \bar{h}_i^o}{M^2}\frac{\partial M}{\partial T} \tag{16}$$

Using Eq. (11)–(15), rearranging Eq. (16) gives:

$$\left(\frac{\partial h}{\partial T}\right)_P = c_{p_g} = \frac{1}{M}\left[\sum_{i=1}^{10} y_i \bar{c}_{p_i} + \frac{\partial y_i}{\partial T}\bar{h}_i^o - \frac{M_T}{M} y_i \bar{h}_i^o\right] \quad [\mathrm{kJ/kgK}]. \tag{17}$$

where

$$M_T = \frac{\partial M}{\partial T} = \sum_{i=1}^{10} M_i \frac{\partial y_i}{\partial T} \tag{18}$$

T is the combustion temperature in Kelvin at which the mole fractions of each equilibrium species, y_i are produced, M_i is the molecular weight of species i, and M is the molecular weight of the mixture as follows :

$$M = \sum_{i=1}^{10} m_i = \sum_{i=1}^{10} y_i M_i \tag{19}$$

From the law of conservation of mass, the mass of the products is equal to the mass of reactants (m_R). A definition can be made as follows:

$$m_R = m_{a1} + m_f + m_s \tag{20}$$

The total number of moles of the products can be found by dividing the mass of reactants into the molecular weight of the combustion products as follows:

$$N = \frac{m_R}{M} \tag{21}$$

Lastly, the number of moles $\upsilon_1, \upsilon_2, \upsilon_3 \ldots \upsilon_{10}$ are obtained from:

$$\upsilon_i = y_i N \tag{22}$$

The mean temperature in the primary zone (T_{cc}) at which the emissions occur can be determined by using the adiabatic flame temperature of dry stoichiometric combustion $T_{ad,dry}$, specific heat of dry combustion $C_{pg,dry}$, mass of dry gases $m_{g,dry}$ ($m_{a1} + m_f$), and temperature, specific heat and mass of injected diluent as follows:

$$T_{CC} = \frac{T_{ad,dry} C_{pg,dry} m_{g,dry} + T_s C_{p,s} m_s}{C_{pg,dry} m_{g,dry} + C_{p,s} m_s} \tag{23}$$

$C_{pg,dry}$ can be found by introducing zero for y in Eq. (7) and using the mass fractions of the products obtained from the dry combustion. T_{CC} is the final temperature of combustion in the primary zone with added H_2O which is necessary to calculate how much extra fuel is needed to reach again the desired TIT for the different injection ratios.

Pressure losses are very important and should also be taken into consideration. Rolls-Royce [63] states that if 5% pressure loss in a turbine can be turned into 5% pressure gain, it has the same impact as doubling the compression ratio.

Taking the pressure loss in the CC into account the value of T_{CC_P} can be reevaluated as follows:

$$T_{CC_P} = T_{CC}(1-\lambda)^{k-1/k} \tag{24}$$

Injected excess fuel increases the overall equivalence ratio and the mean temperature in the combustion chamber which determines the ultimate temperature of the combustor exit gases, TIT, after mixing with the dilution air added gradually before entering the turbine. The fuel/air ratio is adjusted due to the changes in steam and dilution air mass flows in order to maintain a constant TIT at all working conditions and TIT is controlled by the following equation:

$$\mathrm{TIT} = T_3 = \left[T_{CC_P} C_{p_{CC}}\left(m_{g,dry} + m_s\right) + T_2 C_{pa_2} m_{a_2}\right] \Big/ \left[C_{p_{CC}}\left(m_{g,dry} + m_s\right) + C_{pa_2} m_{a_2}\right] \tag{25}$$

Here m_{a2} is the amount of total cooling air which is used to lower the gas temperature before it enters the turbine and C_{pa_2} is the specific heat of air at T_2 defined by using the air properties table [64] and $C_{p_{CC}}$, the constant pressure specific heat corresponding to T_{cc} is obtained from the following relation:

$$C_{p_{CC}} = \left(C_{pg,dry} m_{g,dry} + C_{p,s} m_s\right) \Big/ \left(m_{g,dry} + m_s\right) \tag{26}$$

TIT can also be calculated neglecting the effect of the cooling air in Eq. (25) but taking it as excess air into account when calculating $T_{ad,dry}$.

The heat added in the CC can be calculated as follows where LHV is the lower heating value of the fuel:

$$Q_{in} = \left(m_f \times \mathrm{LHV}\right) \Big/ \eta_{cc} \tag{27}$$

2.3. Expansion analysis

The expansion analysis is similar to the compression analysis and can be made by using the relative pressures Pr_3 and Pr_4 which can be obtained from Eq. (28) as follows:

$$Pr_3(T_3) = \exp\left[\frac{\sum y_i \bar{s}_i^o(T_3)}{\bar{R}_u}\right] \tag{28}$$

and

$$Pr_{4,is} = Pr_3\left[\frac{P_4}{P_3}\right] \tag{29}$$

Taking pressure loss in the CC into account, P_3 can be found from

$$P_3 = (1-\lambda)P_2 \tag{30}$$

where λ is the pressure loss ratio in the CC.

Eq. (28) can be rewritten in the following form for turbine exit conditions and $T_{4,is}$ can be obtained by trial and error from :

$$\bar{s}^o(T_{4,is}) = \sum_{i=1}^{10} y_i \bar{s}_i^o(T_{4,is}) = \bar{R}_u In Pr_{4,is} \tag{31}$$

The actual exhaust gas temperature T_4 can be found by:

$$T_4 = T_3 - \eta_{t,is}(T_3 - T_{4,is}) \tag{32}$$

where $\eta_{t,is}$ is the turbine efficiency which is the ratio of the 'actual work obtained' to the 'maximum work' that could have been obtained by expanding the gas reversibly and adiabatically between the same initial and final pressures.

The exhaust species at chemical equilibrium which are the products of combustion at temperature T_{cc} are cooled to T_4. Consequently the enthalpy of exhaust gases (cooled combustion products) is changed to h_4 and should be determined introducing T_4 into Eq. (11) and using Eq. (15) in order to calculate the specific net work of the turbine as follows:

$$w_t = h_3 - h_4 \tag{33}$$

and the net work output of the overall gas turbine is obtained from subtracting the compressor work and pump work from the turbine work which yields:

$$W_{NET} = m_t w_t - m_a w_c - m_s w_p \tag{34}$$

where

$$m_t = m_a + m_f + m_s \tag{35}$$

The cycle thermal efficiency η_{th} can be found as follows:

$$\eta_{th} = W_{NET}/Q_{in} \tag{36}$$

After obtaining the net specific work, specific fuel consumption, which is an indication of economic performance, can be calculated as below:

$$SFC = \left(3600 m_f 1000\right) \Big/ W_{NET} \quad [\mathrm{g/kWh}]. \tag{37}$$

2.4. Pollutant emissions

While the combustion in a gas turbine is an incomplete process the exhaust products mainly are carbon dioxide (CO_2), water vapor (H_2O), excess atmospheric oxygen (O_2) and nitrogen (N_2). Carbon dioxide and water vapor have not always been regarded as pollutants because they are the natural consequence of complete combustion of a hydrocarbon fuel. However, they both contribute to global warming and can only be reduced by burning less fuel [65].

Legislation pressure on environmental emissions has created extensions on OEMs design staff to lower gas turbine emissions, particularly oxides of nitrogen and carbon monoxide. For a gas turbine engine burning a lean mixture of natural gas and air, the emissions of unburned hydrocarbons (UHC) and sulfur (SO_x) are negligibly small and therefore most regulations for stationary gas turbines have been directed at NO_x and CO [66] and they are being taxed in a growing number of global locations [67].

To calculate NO_x and CO emissions the following semi-empirical equations given by Lefebvre [68] have been used:

$$NO_x = 0.459 \times 10^{-8} P^{0.25} F t_{res} \exp(0.01 T_{pz}) \tag{38}$$

$$CO = 0.333 \times 10^{10} \frac{\exp(-0.00275 T_{pz})}{F P^{1.5} (t_{res} - 0.55 t_{ev}) (\Delta P/P)^{0.5}} \tag{39}$$

Here P is CC pressure in Pascal, F is primary air ratio, T_{pz} is primary zone temperature and t_{ev} is the fuel evaporation time. t_{ev} can be taken as zero for gaseous fuels. $\Delta P/P$ is the dimensionless pressure loss in the CC.

Temperature in the primary zone at which the emissions occur is obtained from the steam injected chemical equilibrium scheme for $\phi = 1.02$. NO_x and CO emissions are obtained as $EINO_x$ and EICO (grams per kilogram of fuel).

Based on the above model a computer program has been developed for multi-criterion optimization of steam injected gas turbine cycles. The results are given in the following section.

3. Results and discussion

A code is developed and simulated in MATLAB to evaluate and optimize the thermo-ecologic performance of the STIG cycle modeled in the previous section. Precision improvement of the proposed model is presented by running the model for TIT = 1300 °C, $\pi_C = 30$ and 5% of steam injection (Case 0). For this specific case, comparisons are made running the same model using some very common assumptions of gas turbine models in the available literature and deviations from the proposed model results caused by those assumptions can be seen in Table 2. Case 1 represents assumption of complete combustion with only four combustion products, Case 2 represents the case when injected steam is assumed as ideal gas and Case 3 is the case when pressure losses are neglected. Four combustion products used in Case 1 are CO_2, H_2O, N_2 and O_2 but when $T_{ad,pri}$ is calculated, CO is used instead of O_2 because of the slightly rich combustion in the primary zone ($\phi = 1.02$). Further, variations of performance parameters with respect to pressure, steam injection and equivalence ratios are illustrated by Figs. 2–13 per unit mass flow rate of working fluid and discussions on the results are presented below:

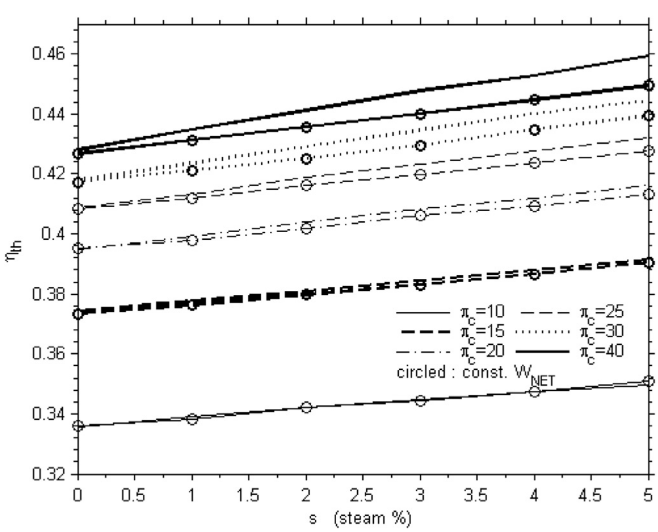

Fig. 2. The change of thermal efficiency versus steam injection ratio at constant TIT and constant net work output.

Fig. 2 shows the change of thermal efficiency versus steam injection ratio for different pressure ratios for constant TIT and constant net work output conditions. At both conditions, the thermal efficiency of gas turbine increases with increasing steam injection ratio. This is because net work output increase is higher than the extra heat addition due to the steam injection for constant TIT conditions. For constant net work output condition, thermal efficiency increases due to the decreasing fuel consumption while net work output remains unchanged. The figure also shows the effect of pressure ratio on thermal efficiency. Thermal efficiency increases with increasing pressure ratio for both constant TIT and net work

output conditions. With increased pressure, combustion chamber inlet temperature increases so less heat i.e. less fuel energy is needed to reach the desired TIT. The effect of pressure ratio on thermal efficiency decreases with increasing pressure ratio. The effect of steam injection on thermal efficiency also increases with increasing pressure ratio. For constant TIT conditions, at pressure ratio 10, 5% of steam injection leads to 4.3% increase in thermal efficiency where this value is 8.1% at pressure ratio 40. At constant net work output conditions, at pressure ratio 10, 5% of steam injection leads to 4.2% increase in thermal efficiency where this value is 5.3% at pressure ratio 40.

Fig. 3 shows the change of net work output versus steam injection ratio at different pressure ratios at constant TIT conditions. With increasing steam injection ratios, the net work output of the gas turbine always increases. Moreover the effect of steam injection on net cycle work also increases with increasing pressure ratio. At pressure ratio 10, 5% of steam injection leads to 14.9% increase in net work output where this value is 22.4% at pressure ratio 40. One can also see that the optimum pressure ratio for the maximum net work output falls between 15 and 25.

Fig. 4a shows the change of fuel energy added during combustion versus steam injection ratio at different pressure ratios for constant TIT and constant net work output conditions. For both conditions fuel energy, i.e. heat added to the system with fuel, decreases with increasing pressure ratio because CC inlet temperature increases with increasing pressure ratio and less fuel energy is needed to reach the desired TIT. For constant TIT conditions, for all pressure ratios injected steam increases the fuel energy added in CC because cooler steam rejects heat from the hot combustion gases and consequently fuel consumption increases. This leads to an increase in heat added to the system. The increase in added heat caused by steam injection decreases slightly with increasing pressure ratios. For constant net work conditions steam injection decreases heat added so the fuel consumption of the system. For increasing pressure ratios this effect slightly decreases as for the constant TIT conditions. At higher pressure ratios, fuel energy needed decreases slower than that of lower pressure ratios with increasing steam injection ratios. Fuel consumption decreases with steam injection at constant net work output conditions because although the specific heat of the working fluid and mass flow rate increases with steam injection, the enthalpy difference between turbine inlet and turbine exit remains same. So TIT can be lowered

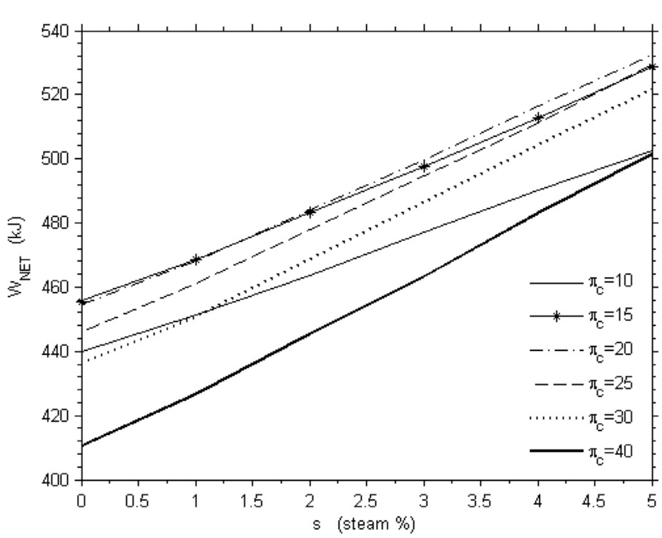

Fig. 3. The change of specific net work output versus steam injection ratio at constant TIT.

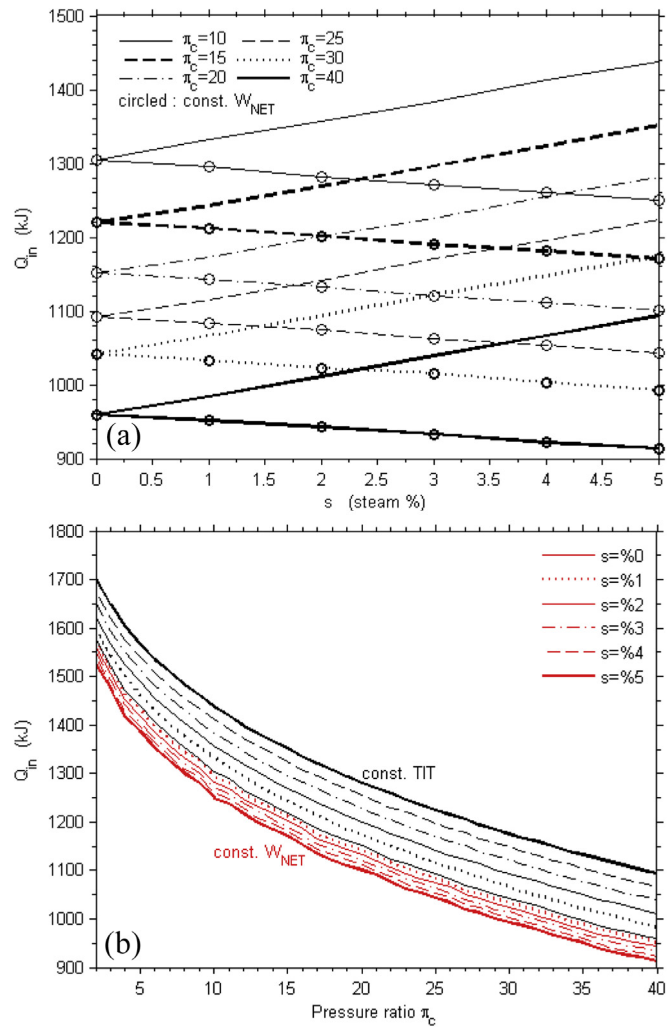

Fig. 4. a: The change of heat added in CC versus steam injection ratio at constant TIT and constant net work output conditions. b: Change of heat added versus pressure ratio at constant TIT and constant net work output conditions.

by decreasing the amount of fuel in the combustion chamber. A lower overall equivalence ratio is enough to maintain a constant net work output during steam injection. A 5% of steam injection decreases the heat added by 4.14% for the constant net work output and increases the heat added by 10.2% for the constant TIT condition.

Fig. 4b shows the change of heat added to the system versus pressure ratio for constant TIT and constant net work output conditions. At both cases increasing pressure ratio increases the compressor outlet temperature which decreases the heat added in the CC. For constant TIT, the heat added increases with steam injection because of the heat rejected by the injected steam and it can be seen that this effect of steam injection increases with increasing pressure ratios. Under constant net work conditions, Q_{in} is lower than that it is under constant TIT conditions which is a sign of lower fuel consumption. The effect of steam injection is contradictory at constant net work output conditions because of the reasons explained for Fig. 4a.

Fig. 5a and b shows change of thermal efficiency and specific fuel consumption versus pressure ratio at different steam injection ratios for constant TIT and constant net work output conditions respectively. As seen in Fig. 2, thermal efficiency increases with steam injection ratio for both conditions. As pressure ratio

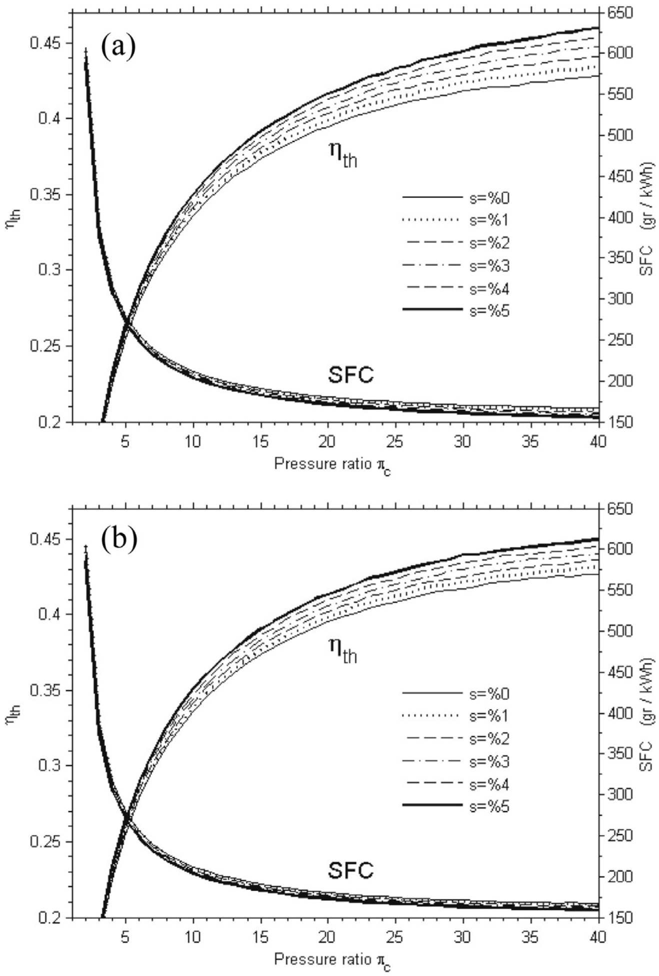

Fig. 5. a The change of thermal efficiency and specific fuel consumption versus pressure ratio at constant TIT. b The change of thermal efficiency and specific fuel consumption versus pressure ratio at constant net work output.

increases, the increase in thermal efficiency gets slower. The increase in thermal efficiency with increasing steam injection decreases slightly at any pressure ratio. The increase in net work output is greater than the increased fuel amount so the specific fuel consumption decreases as the pressure ratio increases. Additionally, as discussed in Figs. 2 and 4, combustion chamber inlet temperature increases with increasing pressure ratio and less fuel energy is needed to reach the desired TIT which also decreases SFC. There is a sharper decrease in SFC at smaller pressure ratios and it decreases more slowly with increasing pressure ratios. At constant TIT conditions SFC is slightly better than the constant net work conditions although fuel consumption is less for the constant net work condition.

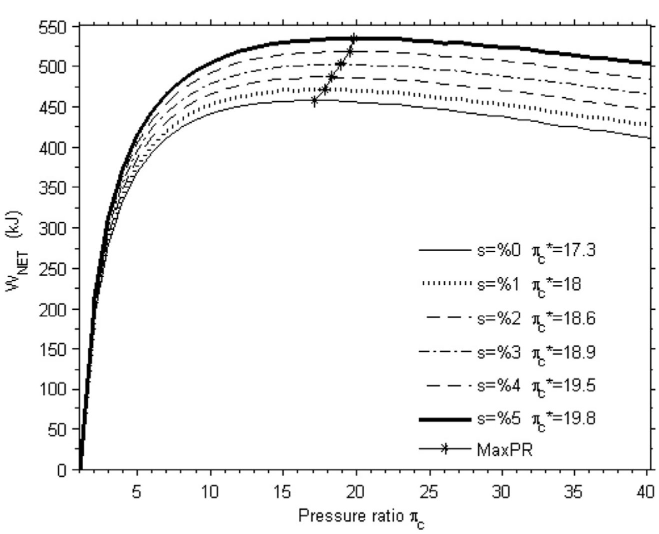

Fig. 6. The change of specific net work output versus pressure ratio at constant TIT.

Fig. 6 shows change of net work versus pressure ratio for different steam injection ratios at constant TIT conditions. The optimum pressure ratios at which the net work output is maximum are shown in the figure with their approximate values. In agreement with Fig. 3, the optimum pressure ratio for maximum work output is about 17 for no injection case. As more diluent is injected this value shifts to the right and for 5% injection, the optimum pressure ratio increases up to 20.

Fig. 7a shows the change of net work output versus thermal efficiency at different steam injection ratios for varying pressure ratios and dedicated equivalence ratios for constant TIT condition

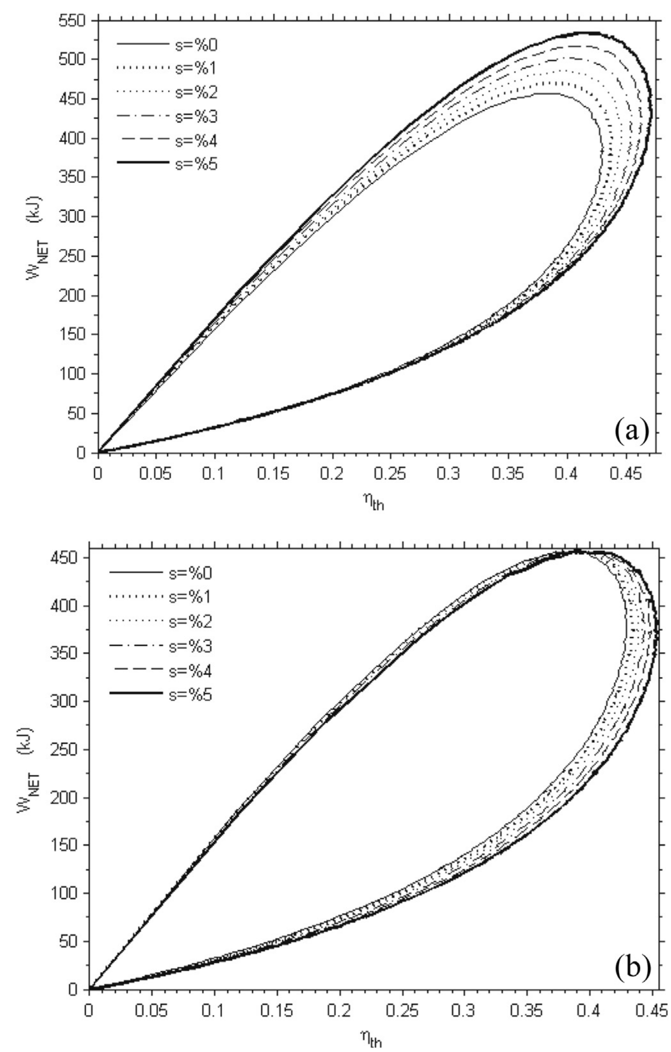

Fig. 7. a: The change of net work output versus thermal efficiency at and effect of steam/water injection at different injection ratios for varying pressure ratios at constant TIT. b: The change of net work output versus thermal efficiency at and effect of steam/water injection at different injection ratios for varying pressure ratios at constant net work output.

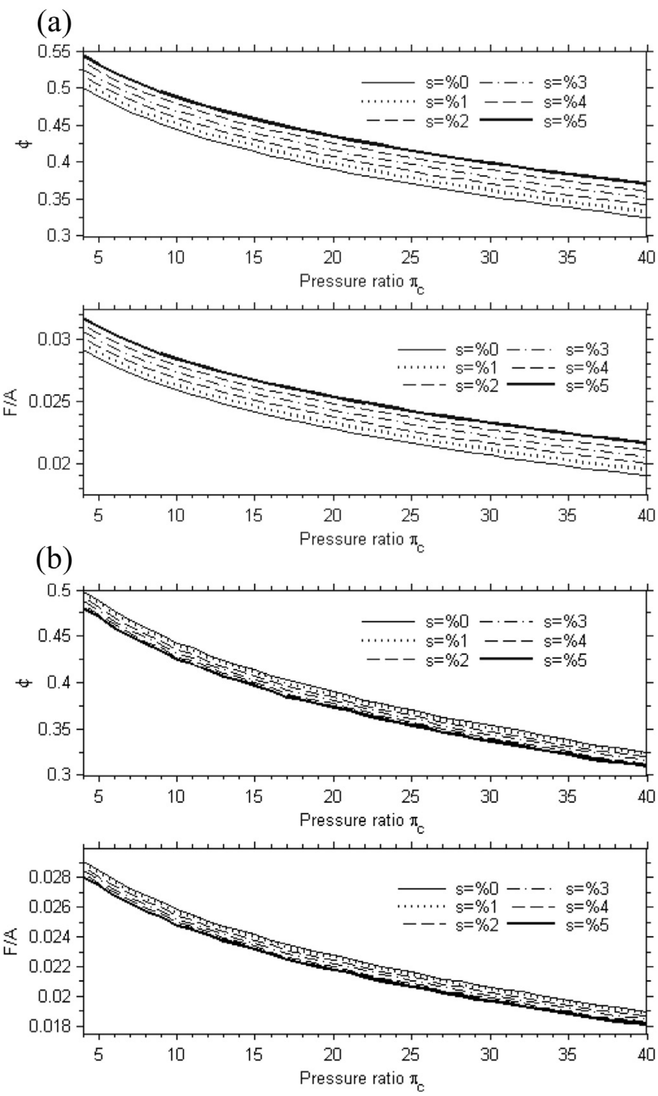

Fig. 8. a: The change of equivalence and fuel/air ratio versus pressure ratio for different steam injection ratios at constant TIT. b: The change of equivalence and fuel/air ratio versus pressure ratio for different steam injection ratios at constant net work output.

where Fig. 7b is for the constant net work output condition. Both for injection and no-injection case the net work output and the thermal efficiency increases with increasing pressure ratio up to their maximum values. At pressure ratios higher than the pressure ratio corresponding to their maximum value, the net work and efficiency start to decrease. At constant net work output conditions which is shown in Fig. 7b, values of maximum net work and thermal efficiency are lower at all rates of steam injection. All loops which represent different rates of steam injection are intersecting at the maximum net work point. It is observed that after the pressure ratio corresponding to the maximum net work conditions, the effect of steam injection on the net cycle work decreases whereas the effect on the thermal efficiency increases.

Fig. 8a and b shows the change of equivalence and fuel/air ratio versus pressure ratio for different steam injection ratios for constant TIT and constant net work output conditions respectively. As equivalence ratio is a measure of fuel/air ratio, both graphs have the same tendency towards steam injection and pressure ratio. As pressure ratio increases the equivalence ratio and fuel/air ratio decreases because the temperature at the end of compression increases with increasing pressure ratio which helps in consumption of less fuel in the combustion chamber. On the contrary, as the steam injection ratio increases they both increase because steam being cooler than the burned gases rejects heat from the combustion chamber, so more fuel is needed to reach the desired temperatures. At constant net work conditions it can be seen that equivalence ratio and dedicated FA ratio is less which is a sign of less fuel requirement.

Fig. 9 shows the change of primary air ratio F used in Eqs. (38) and (39) with increasing steam injection ratios to reach the desired TIT value for both constant TIT and constant net work output conditions. The values are calculated with regards to the overall FA ratio. For constant TIT conditions, as more steam is injected more fuel should be added to the combustion which also requires more air to maintain near-stoichiometric combustion where $\phi = 1.02$. For this reason the percentage of the total air used for combustion increases with increasing steam injection and decreasing pressure ratios i.e. the percentage of the dilution air decreases while TIT is held constant at its desired value. For the constant net work output condition F decrease because less fuel is needed for the near-stoichiometric combustion.

Fig. 10 shows the effect of steam injection on CO and NO_x emissions with increasing pressure ratio. Amount of pollutants are given in grams per kg-fuel basis for no injection and 5% of steam injection cases. CO and NO_x emissions are affected adversely by changes of flame temperature. There is a slight increase in CO with steam injection and significant decrease with increasing pressure ratios. This is because the flame temperature in the primary zone increases with pressure ratio due to the increasing inlet air temperature. On the other hand NO_x decreases with steam injection and increases with increasing pressure ratio because of the increasing combustion inlet temperature at higher pressure ratios.

For Figs. 11–13 equivalence ratios are the overall equivalence ratios, i.e. all the air after the compression, is assumed to take part in the combustion process and TIT is not held constant and increases due to the increase in equivalence ratios and pressure ratios. TIT is not held constant and is allowed to increase with increasing pressure and equivalence ratios much above the metallurgical limits. For each equivalence ratio, TIT is assumed to be equal to the adiabatic flame temperature after pressure loses.

Fig. 11 shows the change of thermal efficiency for maximum net work conditions for varying equivalence and steam injection ratios and puts theoretical limits of the steam injected gas turbine cycle for the given conditions. Here, pressure ratio is parametrically increased to seek for the theoretically achievable maximum net work. As TIT is not held constant, calculated theoretical cycle thermal efficiency is much higher than that of the state of the art gas turbine engines. There is a continuous increase in the maximum net work output and corresponding thermal efficiency both together at all steam injection ratios up to the overall equivalence ratio $\phi = 0.8$. After that, the maximum net work keeps increasing but corresponding thermal efficiency decreases. The reason of this decrease is a higher increase in fuel amount than the corresponding increase in net work output. For lower equivalence ratios, thermal efficiency is more affected by steam injection as the graph gets wider rightwards. The effect of steam injection on maximum net work is negligible but increasing with increasing equivalence ratios.

Fig. 12 shows the change of net work versus thermal efficiency at different equivalence and steam injection ratios for the selected pressure ratio of 30. TIT is not held constant and increases due to the increase in equivalence ratio. It is assumed to be equal to the adiabatic flame temperature after pressure loses. As seen in the figure, net work of the cycle increases with equivalence ratio. For all injection cases the thermal efficiency makes a peak at overall

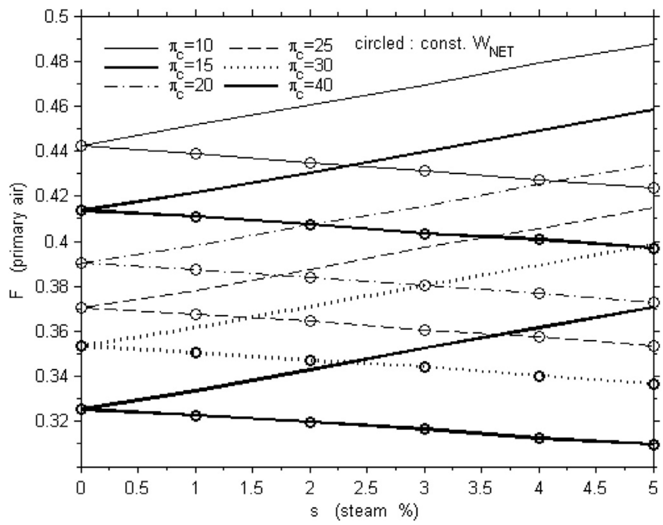

Fig. 9. The change of primary air ratio with increasing steam injection ratios at constant TIT and constant net work output.

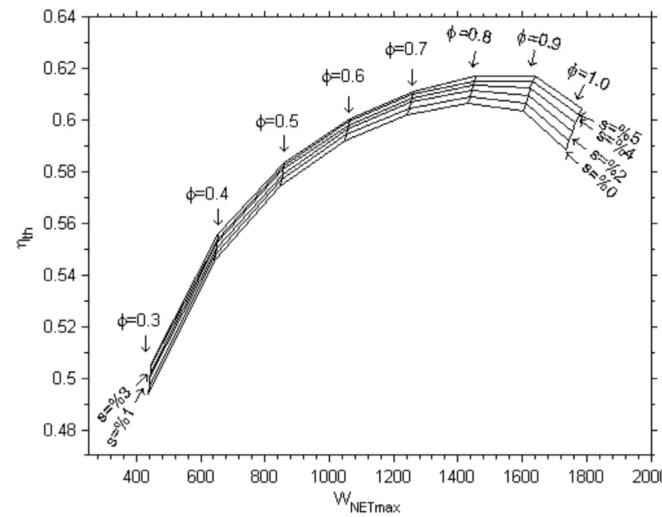

Fig. 11. Thermal efficiency for the maximum net work conditions for varying equivalence and steam injection ratios, steam at 300 °C at constant TIT.

equivalence ratio of 0.8. After this equivalence ratio, thermal efficiency decreases. The effect of steam injection on net work output is negligible but increases with increasing equivalence ratios. There is a slight decrease in net work output mostly due to decreasing TIT and slightly due to increasing pump work for increasing injection ratios.

Fig. 13 shows the change of turbine inlet temperature versus thermal efficiency at different equivalence ratios and steam injection ratios at pressure ratio 30. Equivalence ratios are again the overall equivalence ratios, so the figure approximates how much the injected steam decreases the flame temperature for different injection ratios. The effect of equivalence ratio on the TIT decreases with increasing equivalence ratios as gaps between equivalence ratios gets narrower on the graph. Knowing that when the flame temperature exceeds 1800 K, a decrease of 30–70 K in peak flame temperature can decrease NO formation by half [69] this figure also gives an intuition for the NO_x emissions at the turbine exit.

4. Conclusion

Gas turbines are widely used in industry and meet an important portion of world's total energy demand. Their economic and ecological performance improvement has been a significant concern. This paper gives a precise approach on gas turbine engine simulation combining two key objectives: performance evaluation and emission optimization. It addresses the different gas turbine models in the available literature and proposes a more precise model which depends on the exact properties of the combustion products. Effects of each improvement on the net work output, thermal efficiency, adiabatic flame temperature and pollutant emissions are tabulated for a specific case. The steam injected gas turbine model is run for different pressure ratios for parametric analysis and also for the specific pressure ratio $\pi_C = 30$ and 5% of steam injection.

Constant TIT and constant net work output conditions are compared for net work output, thermal efficiency and fuel consumption and optimum working conditions are identified.

For the constant TIT condition, it was observed that although net work of the cycle decrease after an optimum pressure ratio, the effect of steam injection on the net cycle work and thermal

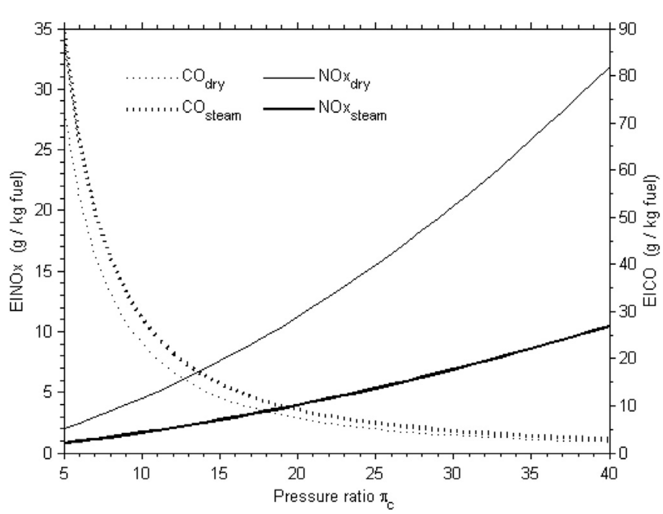

Fig. 10. The change of $EINO_x$ and EICO with 5% of steam injection at different pressure ratios at constant TIT.

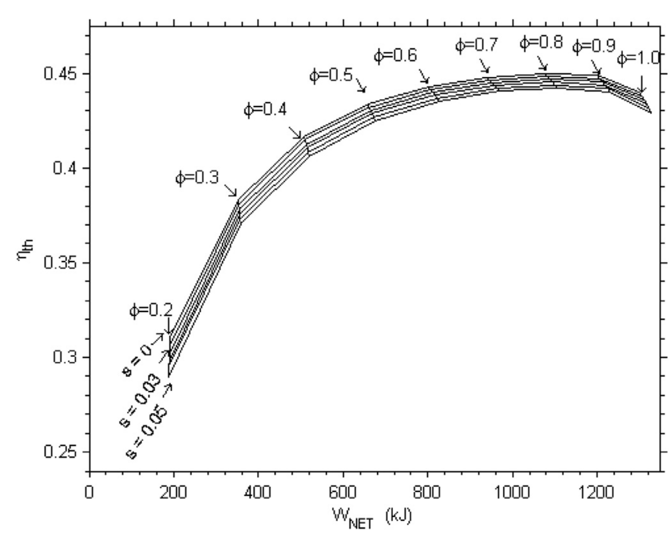

Fig. 12. Carpet plot showing the change of net specific work versus thermal efficiency at different equivalence ratios and steam injection ratios, steam at 300 °C $Pr = 30$ at constant TIT.

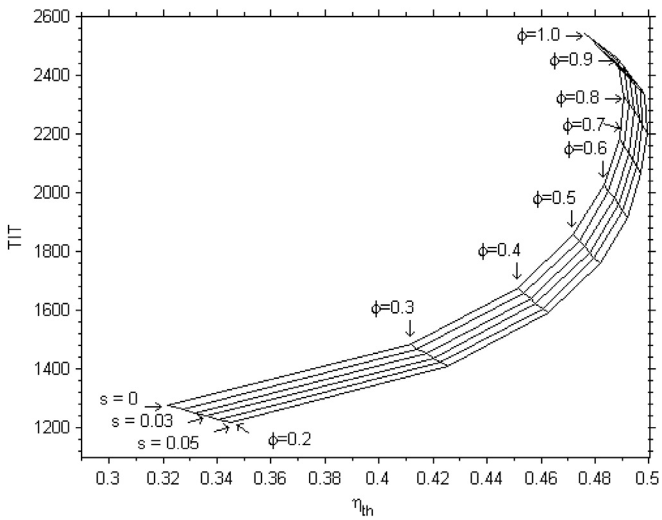

Fig. 13. Carpet plot showing the change of turbine inlet temperature versus thermal efficiency at different equivalence ratios and steam injection ratios, steam at 300 °C $Pr = 30$.

efficiency increases with increasing pressure ratio. For the proposed gas turbine, 5% of steam/air ratio increased the gas turbine thermal efficiency about 15% for pressure ratios of 10 and about 20% for pressure ratios of 40.

At optimum pressure ratios for the maximum net work output, net work is increased by 17%. Another observation was the increasing fuel consumption although the thermal efficiency of the cycle increases. This means for the constant work output condition, a steam injected gas turbine cycle will consume less fuel and will be more environmental friendly producing less pollutants and less CO_2 which contributes global warming. While decreasing the fuel consumption, running the steam injected cycle for constant net work output decreases the cycle thermal efficiency. At pressure ratio of 40, thermal efficiency decreases from 45.95% to 44.69% at pressure ratio 40.

For constant TIT conditions, at pressure ratio 10, 5% of steam injection leads to 4.3% increase in thermal efficiency where this value is 8.1% at pressure ratio 40. At constant net work output conditions, at pressure ratio 10, 5% of steam injection leads to 4.2% increase in thermal efficiency where this value is 5.3% at pressure ratio 40.

Fuel consumption changes significantly for the cases of constant TIT and constant net work output. 5% of steam injection increases fuel consumption by about 11.3% and decreases fuel consumption by about 4.5% for each case respectively at any pressure ratio. Another observation is steam injection increases the optimum pressure ratio for the maximum net work. Optimum pressure ratio for maximum net work is increased from 17.3% to 19.8% with increasing steam injection form 0%–5% for constant TIT condition. For constant net work output condition, optimum pressure ratio for maximum net work is found to be 15 and is not affected by steam injection.

The proposed model can directly be used for dry or water injected gas turbines for any fuel chemistry. The modeling procedure is easily adaptable to many future gas turbine studies such as alternative fuel or multi-fuel studies and EGR applications of gas turbines with or without H_2O injection or any kind of diluents. Advanced gas turbines cycles with intercooling, reheat and regeneration or combined cycles can also be evaluated in the same manner. With its precision and speed it is a fast and effective tool that can safely be used for parametrical analysis of various gas turbine models. It also provides the necessary data for the economic analysis of gas turbines.

Acknowledgements

This work is derived from authors unpublished Ph.D. Thesis: “Effects of water/steam injection on the thermo-economic performance and emissions of gas turbines and their optimization”. The authors wish to thank Şaban Pusat from Yıldız Technical University for his time and valuable assistance. The authors also wish to express their sincere gratitude to George Richards from United States Department of Energy and Prof. Yiguang Ju from Princeton University for their valuable comments on this study.

Nomenclature

C	specific heat [kJ/kg K]
CC	combustion chamber
EGR	exhaust gas recirculation
F	primary air ratio
FA	fuel/air ratio
h	specific enthalpy [kJ/kg]
H	enthalpy [kJ]
HRSG	heat recovery steam generator
ISO	International Standards Organization
k	isentropic exponent [C_p/C_v]
MW	molecular weight
N	total number of moles of the species
OEM	original equipment manufacturer
Pr	relative pressure
Q	heat [kJ]
q	specific heat [kJ/kg]
R_u	universal gas constant [kJ/kg]
s	steam injection ratio or entropy [kJ/kg K]
SFC	specific fuel consumption
STIG	steam injected gas turbine
T	temperature
TIT	turbine inlet temperature
W	work [kJ]
w	specific work [kJ/kg]
WSR	well-stirred reactor
x	molar injection ratio

Subscripts

1,2,3,4	depicted in Fig. 1
a	air
ad	adiabatic
c	compressor
cc	combustion chamber
e	equilibrium
f	fuel
i	exhaust species
is	isentropic
n	number of components
p	pressure
s	steam, stoichiometric
t	turbine
th	thermal
u	unburned

Superscripts

—	per mole, molar
·	flowrate
o	standard reference state, 25 °C, 1 atm.

Greek letters

α	number of carbon atoms
β	number of hydrogen atoms
δ	number of oxygen atoms
ε	molar air–fuel ratio
ϕ	equivalence ratio
γ	number of nitrogen atoms
λ	pressure loss factor
η	efficiency
π	pressure ratio
ν	specific volume [m^3/kg]

Appendix A. Supplementary data

Supplementary data associated with this article can be found in the online version, at http://dx.doi.org/10.1016/j.applthermaleng.2014.06.052.

References

[1] D.F. Woodyard, Pounder's Marine Diesel Engines and Gas Turbines, ninth ed., Elsevier/Butterworth-Heinemann, Oxford, UK, 2009.
[2] O.A. Training, Gas Turbine Engines for the Airline Transport Pilot's Licence, OATmedia, Kidlington, 2006.
[3] M. Moliere, Expanding fuel flexibility of gas turbines, J. Power Energy 219 (A2) (2005) 109–119.
[4] T.G. Koivu, New technique for steam injection (STIG) using once through steam generator (GTI/OTSG) heat recovery to improve operational flexibility and cost performance, in: 17th Symposium on Industrial Application of Gas Turbines (IAGT) Banff, Alberta, Canada, 2007. Paper No: 07-IAGT-2.2.
[5] B.N. Sanneman, Pioneering gas turbine-electric system in cruise ships: a performance update, Mar. Technol. SNAME News 41 (4) (2004) 161–166.
[6] F. Bozza, R. Tuccillo, G. Fontana, Performance and emission levels in gas-turbine plants, J. Eng. Gas Turb. Power 116 (1) (1994) 53–62.
[7] W.P.J. Visser, S.C.A. Kluiters, Modelling the Effects of Operating Conditions and Alternative Fuels on Gas Turbine Performance and Emissions, vol. NLR-TP-98629, NLR National Aerospace Laboratory, Netherlands, 1998.
[8] A. Bouam, S. Aissani, R. Kadi, Evaluation of gas turbine performances and NO_x and CO emissions during the steam injection in the upstream of combustion chamber, in: Syrian Renewable Energy Conference ICRE 2010, 2010, pp. 1–6.
[9] R. Kurz, Gas turbine performance, in: 34th Turbomachinery Symposium San Diego, California, 2005, pp. 131–146.
[10] A. Bouam, S. Aissani, R. Kadi, Combustion chamber steam injection for gas turbine performance improvement during high ambient temperature operations, J. Eng. Gas Turb. Power 130 (4) (2008).
[11] K.H. Kim, Effects of Water and Steam Injection on Thermodynamic Performance of Gas Turbine Systems, vol. 110–116, Trans. of Technical Publications, 2011, pp. 2109–2116.
[12] R.J. Boyle, Effect of Steam Addition on Cycle Performance of Simple and Recuperated Gas Turbines, National Aeronautics and Space Administration, Washington Springfield, VA, 1979.
[13] M. Yari, K. Sarabchi, Modelling and optimization of part-flow evaporative gas turbine cycles, P I Mech. Eng. A-J Pow. 219 (A7) (2005) 533–548.
[14] Y.H. Zhu, H.C. Frey, Simplified performance model of gas turbine combined cycle systems, J. Energy Eng-Trans ASCE 133 (2) (2007) 82–90.
[15] A. Bouam, S. Aissani, R. Kadi, Gas turbine performances improvement using steam injection in the combustion chamber under sahara conditions, Oil Gas Sci. Technol. 63 (2) (2008) 251–261.
[16] B. Sheikhbeigi, M.B. Ghofrani, Thermodynamic and environmental consideration of advanced gas turbine cycles with reheat and recuperator, Int. J. Environ. Sci. Technol. 4 (2) (2007) 253–262.
[17] J.J. Lee, D.W. Kang, T.S. Kim, Development of a gas turbine performance analysis program and its application, Energy 36 (8) (2011) 5274–5285.
[18] K.H. Kim, G. Kim, Thermodynamic performance assessment of steam injection gas turbine systems, World Acad. Sci. Eng. Technol. 68 (2010) 1137–1143.
[19] K. Mathioudakis, Evaluation of steam and water injection effects on gas turbine operation using explicit analytical relations, J. Power Energy 216 (A6) (2002) 419–431.
[20] Q.Z. Al-Hamdan, M.S.Y. Ebaid, Modeling and simulation of a gas turbine engine for power generation, J. Eng. Gas Turb. Power 128 (2) (2006) 302–311.
[21] M. Cardu, M. Baica, Gas turbine installation with total water injection in the combustion chamber, Energy Convers. Manag. 43 (17) (2002) 2395–2404.
[22] M.M. Alhazmy, Y.S.H. Najjar, Augmentation of gas turbine performance using air coolers, Appl. Therm. Eng. 24 (2–3) (2004) 415–429.
[23] H.B. Avval, et al., Thermo-economic-environmental multiobjective optimization of a gas turbine power plant with preheater using evolutionary algorithm", Int. J. Energy Res. 35 (5) (2011) 389–403.
[24] T.H. Fransson, CompEduHPT: Computerized Educational Platform in Heat and Power Technology, Department of Energy Technology, KTH, Sweden, 2003.
[25] S.C. Gulen, A simple parametric model for the analysis of cooled gas turbines, J. Eng. Gas Turb. Power 133 (1) (2011).
[26] O.O. Badran, Gas-turbine performance improvements, Appl. Energy 64 (1–4) (1999) 263–273.
[27] A. De Sa, S. Al Zubaidy, Gas turbine performance at varying ambient temperature, Appl. Therm. Eng. 31 (14–15) (2011) 2735–2739.
[28] S.M. Seyyedi, H. Ajam, S. Farahat, Thermoenvironomic optimization of gas turbine cycles with air preheat, J. Power Energy 225 (A1) (2011) 12–23.
[29] W.E. Fraize, C. Kinney, Effects of steam injection on the performance of gas-turbine power cycles, J. Eng. Power-Trans. ASME 101 (2) (1979) 217–227.
[30] A.H. Lefebvre, Fuel effects on gas-turbine combustion-liner temperature, pattern factor, and pollutant emissions, J. Aircr. 21 (11) (1984) 887–898.
[31] J. Odgers, D. Kretschmer, The Prediction of Thermal NO_x in Gas Turbines, ASME Paper 85-IGT-126, 1985.
[32] G.D. Lewis, A new understanding of NO_x formation, in: Tenth International Symposium on Air-breathing Engines, vol. 91, ISABE, Nottingham, UK, 1991, pp. 625–629.
[33] N.K. Rizk, H.C. Mongia, Semianalytical correlations for NO_x, CO, and UHC emissions, J. Eng. Gas Turb. Power 115 (3) (1993) 612–619.
[34] A. Lazzaretto, A. Toffolo, Energy, economy and environment as objectives in multi-criterion optimization of thermal systems design, Energy 29 (8) (2004) 1139–1157.
[35] O.L. Gulder, Flame temperature estimation of conventional and future jet fuels, J. Eng. Gas Turb. Power 108 (2) (1986) 376–380.
[36] J.B. Heywood, Internal Combustion Engine Fundamentals, McGraw-Hill, New York, US, 1988.
[37] M. Rashidi, Calculation of equilibrium composition in combustion products, Appl. Therm. Eng. 18 (3–4) (1998) 103–109.
[38] C.D. Rakopoulos, et al., A fast algorithm for calculating the composition of diesel combustion products using 11 species chemical-equilibrium scheme, Adv. Eng. Softw. 19 (2) (1994) 109–119.
[39] C. Olikara, G.L. Borman, A Computer Program for Calculating Properties of Equilibrium Combustion Products with Some Applications to I.C. Engines, Society of Automotive Engineers, Warrendale, PA, 1975.
[40] C.R. Ferguson, Internal Combustion Engines: Applied Thermosciences, John Wiley, New York, 1986.
[41] C. Morley, GASEQ, A Chemical Equilibrium Program for Windows Ver. 0.79, 2005.
[42] CHEMKIN Pro Release 15083, Reaction Design, San Diego, CA, 2009.
[43] H.K. Kayadelen, Y. Üst, Prediction of equilibrium products and thermodynamic properties in H_2O injected combustion for CHON type fuels, Fuel 113 (2013) 389–401.
[44] G. Gonca, Investigation of the effects of steam injection on performance and NO emissions of a diesel engine running with ethanol–diesel blend, Energy Convers. Manag. 77 (1) (2014) 450–457.
[45] H.K. Kayadelen, Y. Ust, Computer simulation of steam/water injected gas turbine engines, in: MCS-8 Eighth Mediterranean Combustion Symposium, The Combustion Institute & International Centre for Heat and Mass Transfer (ICHMT), Izmir, Turkey, 2013.
[46] G. Kokkulunk, et al., Theoretical and experimental investigation of diesel engine with steam injection system on performance and emission parameters, Appl. Therm. Eng. 54 (1) (2013) 161–170.
[47] S. Bahrami, A. Ghaffari, M. Thern, Improving the transient performance of the gas turbine by steam injection during frequency dips, Energies 6 (10) (2013) 5283–5296.
[48] I. Cesur, et al., The effects of electronic controlled steam injection on spark ignition engine, Appl. Therm. Eng. 55 (1–2) (2013) 61–68.
[49] S. Eshatia, et al., Influence of water–air ratio on the heat transfer and creep life of a high pressure gas turbine blade, Appl. Therm. Eng. 60 (1–2) (2013) 335–347.
[50] I. Roumeliotis, K. Mathioudakis, Evaluation of water injection effect on compressor and engine performance and operability, Appl. Energy 87 (4) (2010) 1207–1216.
[51] J.J. Lee, M.S. Jeon, T.S. Kim, The influence of water and steam injection on the performance of a recuperated cycle microturbine for combined heat and power application, Appl. Energy 87 (4) (2010) 1307–1316.
[52] M.P. Boyce, Gas Turbine Engineering Handbook, fourth ed., Elsevier, U.S, 2012.
[53] H. Cohen, et al., Gas Turbine Theory, fourth ed., Longman, Burnt Mill, Harlow, England, 1996.
[54] A. Poullikkas, An overview of current and future sustainable gas turbine technologies, Renew. Sustain. Energy Rev. 9 (5) (2005) 409–443.
[55] A. Tsalavoutas, et al., Correlations adaptation for optimal emissions prediction, in: ASME Turbo Expo '07, ASME, Montreal, Canada, 2007, pp. 1–11.
[56] R. Kadi, A. Bouam, S. Aissani, Analyze of gas turbine performances with the presence of the steam water in the combustion chamber, in: Revuedes Energies Renouvelables, ICREDS, 2007, pp. 327–335.
[57] F.J. Brooks, GE Gas Turbine Performance Characteristics GER-3567h, GE Power Systems, Schenectady, NY, US, 2008.
[58] Y.A. Çengel, M.A. Boles, Thermodynamics: An Engineering Approach, seventh ed., McGraw-Hill, New York, US, 2011.
[59] M.J. Moran, H.N. Shapiro, D.D. Boettner, Fundamentals of Engineering Thermodynamics, seventh ed., Wiley, Hoboken, N.J., US, 2011.
[60] E.L. Keating, Applied Combustion, second ed., CRC Press/Taylor & Francis, Boca Raton, FL, US, 2007.

[61] S.R. Turns, An Introduction to Combustion: Concepts and Applications, second ed., WCB/McGraw-Hill, Boston, 2000.
[62] K. Meintjes, A.P. Morgan, Performance of algorithms for calculating the equilibrium composition of a mixture of gases, J. Comput. Phys. 60 (2) (1985) 219–234.
[63] G.A. Richards, New Developments in Combustion Technology – Part II: Step Change in Efficiency, Princeton, NJ, US, 2012.
[64] S.R. Turns, D.R. Kraige, Property Tables for Thermal Fluids Engineering: SI and U.S. Customary Units, Cambridge University Press, New York, NY, 2007.
[65] A.H. Lefebvre, D.R. Ballal, Gas Turbine Combustion: Alternative Fuels and Emissions, third ed., CRC Press, Boca Raton, FL, US, 2010.
[66] U. Honegger, Gas Turbine Combustion Modeling for a Parametric Emissions Monitoring System (M.Sc. Thesis), Kansas State University, Manhattan, US, 2007.
[67] C. Soares, Gas Turbines A Handbook of Air, Land, and Sea Applications, Butterworth-Heinemann, Oxford, UK, 2008.
[68] F. Casella, C. Mafezzoni, Modelling of NO_x and CO emissions of a small gas turbine unit based on operational data neural networks, in: IFAC Power Plants and Power Systems Control, Elsevier, Seul, Korea, 2003, pp. 115–120.
[69] S. McAllister, J.Y. Chen, A.C.F. Pello, Fundamentals of Combustion Process, Springer, New York, US, 2011.